biologia plantarum
an international journal for experimental botany

BIOLOGIA PLANTARUM (2021) 65: 221-236 DOI: 10.32615/bp.2021.010

The effect of *Fusarium culmorum* inoculation and deoxynivalenol application on proteome response in wheat cultivars Sumai 3 and SW Kadrilj

K. KOSOVÁ[1,*], J. CHRPOVÁ[1], J. ŠANTRŮČEK[2], R. HYNEK[2], M. KLÍMA[1], I.T. PRÁŠIL[1], P. VÍTÁMVÁS[1]

[1] *Division of Crop Genetics and Breeding, Crop Research Institute, Drnovská 507, 161 06 Prague 6, Czech Republic*
[2] *Department of Biochemistry and Microbiology, University of Chemistry and Technology, Technická 3, 160 00 Prague 6, Czech Republic*

[*] Corresponding author: E-mail: kosova@vurv.cz

Abstract

Fusarium head blight (FHB) represents a damaging disease of cereal spikes caused by mycotoxin-producing *Fusarium* fungi revealing adverse effects on grain quality and yield. Chinese spring wheat (*Triticum aestivum* L.) cv. Sumai 3 represents a major source of FHB resistance thanks to *Fhb1* QTL on 3BS chromosome conferring resistance to FHB and encoding a lectin-like protein. The aim of our study lied in a comparison of proteome response to *Fusarium culmorum* inoculation and mycotoxin deoxynivalenol (DON) application at 10 d after inoculation (dai) in spikes of resistant wheat cultivar Sumai 3 and susceptible wheat cultivar SW Kadrilj. Proteome analysis revealed profound impact of *Fusarium* inoculation and mycotoxin application on plant energy metabolism. *Fusarium* inoculation decreased photosynthesis and ATP biosynthesis and increased the level of stress-protective proteins (chaperones such as Hsc70, lectins). Genotype related differences observed at 10 dai indicated an active acclimation in Sumai 3 as indicated by increased content of some enzymes involved in phenolics biosynthesis (phenylalanine ammonia lyase PAL, BAHD acyltransferase), jasmonate biosynthesis (lipoxygenase LOX), and oligosaccharide biosynthesis (sucrose synthase SuSy, UDP-glucose uridylyltransferase) which are an important part of glycoproteins such as lectins and other pathogen-responsive biomolecules. The study thus provides data on plant acclimation to *Fusarium* infection which may underlie superior resistance of Sumai 3 cultivar.

Keywords: deoxynivalenol, energy metabolism, FHB resistance, *Fusarium culmorum*, protective proteins biosynthesis, proteomic analysis, stress-related proteins, *Triticum aestivum*.

Introduction

Fusarium head blight (FHB), also known as scab, represents a serious disease to cereal spikes and developing grains. It is caused by fungi from the genus *Fusarium*, predominantly *Fusarium culmorum* and *Fusarium graminearum*. The fungal pathogens cause losses of grain yield and reveal adverse effects on grain quality due to trichothecene mycotoxin (deoxynivalenol DON; nivalenol NIV) production and their accumulation in developing grains (reviewed in Kosová *et al.* 2009).

Cereals induce an active response to *Fusarium*

Received 8 October 2020, *last revision* 27 January 2021, *accepted* 12 February 2021.
Abbreviations: ALDO - aldolase; APX - ascorbate peroxidase; BAHD-AT - BAHD acyltransferase; CA - carbonic anhydrase; CAT - catalase; dai - days after inoculation; EF1γ2 - elongation factor 1γ2; GAPDH - glyceraldehyde-3-phosphate dehydrogenase; GS - glutamine synthase; GST - glutathione-S-transferase; Hsc70 - heat shock cognate protein 70; LOX - lipoxygenase; MDAR - monodehydroascorbate reductase; mt - mitochondrial isoform; PAL - phenylalanine ammonia lyase; PGK - phosphoglycerate kinase; PGM - 2,3-bisphosphate phosphoglycerate mutase; PRK - phosphoribulokinase; RCA - RubisCO activase A; RubisCO LSU - ribulose-1,5-bisphosphate carboxylase/oxygenase large subunit; SHMT - serine hydroxymethyltransferase; SuSy - sucrose synthase; TCA - tricarboxylic acid cycle; UDPG phosphorylase - UTP - glucose-1-phosphate uridylyltransferase.
Acknowledgements: The work was supported by the institutional project of Czech Ministry of Agriculture MZe CR RO0418 and the projects by Czech Ministry of Agriculture QK1710302 and QK1910269.
Conflict of interest: The authors declare that they have no conflict of interest.

pathogens aimed at elimination of pathogen spreading. Besides agronomical practices to eliminate *Fusarium* spreading, mapping of genetic variability within wheat gene pool can be exploited to identify major quantitative trait loci (QTLs) underlying *Fusarium* resistance. The following types of FHB resistance were described by Mesterházy (1995, 2002): type I. resistance to *Fusarium* invasion; type II. resistance to spreading; type III. resistance to kernel infection; type IV. tolerance; type V. resistance to toxin accumulation; type VI. resistance to late blighting, and type VII. resistance to head death above infection site.

Sumai 3, a Chinese spring wheat cultivar, represents an important source of resistance to FHB which was employed in a wide range of studies aimed at FHB research. Li *et al.* (2001) found enhanced content of chitinases and β-1,3-glucanases in Sumai 3 with respect to its susceptible mutant. Four major QTLs conferring resistance to FHB located on 2DS, 3BS, 6BS, and 5AL chromosomes were mapped in the crosses between Sumai 3 and susceptible wheat cultivars (Waldron *et al.* 1999, Anderson *et al.* 2001, Buerstmayr *et al.* 2002, 2003, Yang *et al.* 2013). The *Fhb1* QTL on 3BS conferring type II resistance to FHB revealed a Mendelian type of inheritance (Cuthbert *et al.* 2006). Recently, a pore-forming toxin-like (PFT) gene conferring FHB resistance at *Fhb1* locus was mapped in Sumai 3 by Rawat *et al.* (2016). PFT was predicted to encode a chimeric lectin with two agglutinin domains and one ETX/MTX2 toxin domain (Rawat *et al.* 2016).

Plant proteomic studies reveal that a given protein could adopt a variety of biological functions depending on its context, i.e., protein isoform or posttranslational modification, cellular localization, and protein and non-protein interacting partners (reviewed in Kosová *et al.* 2018). Since proteins are directly involved in plant resistance to pathogens, study of wheat response to *Fusarium* artificial inoculation and mycotoxin DON artificial application at proteome level represents an important means to understand molecular mechanisms underlying cereal resistance to FHB. Several proteomic studies on *Triticeae* response to *Fusarium* infection were published (Wang *et al.* 2005, Yang *et al.* 2010a, b, Eggert and Pawelczik 2011, Eggert *et al.* 2011, Kosová *et al.* 2017) including wheat FHB-resistant genotypes (Gunnaiah *et al.* 2012, Zhou *et al.* 2005), FHB-susceptible genotypes (Chetouhi *et al.* 2015, Zhou *et al.* 2006) or both (Ding *et al.* 2011) as reviewed by Yang *et al.* (2013); recently, a 2-DE study on wheat phosphoproteome in response to FHB disease was published by Ding *et al.* (2016), a 2-DE study comparing the effect of *Fusarium graminearum* inoculation in young spikes of resistant wheat cv. Sumai 3 *vs.* susceptible cv. Huaimai 27 was published by Ding *et al.* (2017), and a gel-free study comparing proteome response to *F. graminearum* infection in rachides in ten FHB resistant wheat c*vs*. including Sumai 3 and six FHB susceptible c*vs*., was published by Liu *et al.* (2019). By comparison of FHB-resistant and FHB-susceptible wheat genotypes, Liu *et al.* (2019) identified a group of 3 LEA proteins as a marker of FHB resistance and a purple acid phosphatase (PAP) as a marker of FHB susceptibility in wheat.

The aim of our study was to compare response at proteome level to *F. culmorum* infection and DON artificial application in young spikes of wheat FHB-resistant cv. Sumai 3 *vs.* susceptible cv. SW Kadrilj using a two-dimensional difference gel electrophoresis (2D-DIGE) approach followed by a liquid chromatography with tandem mass spectrometry (LC-MS/MS) identification of differentially abundant protein spots. Young green spikes of greenhouse-grown plants were inoculated by *F. culmorum* or sprayed with DON solution at flowering and then sampled for proteomic analysis 10 d after the inoculation (dai). Proteomic analysis was accompanied by basic physiological characterisation of the extent of *Fusarium* infection and determination of DON content in mature grains.

Materials and methods

Plants and treatments: Wheat (*Triticum aestivum* L.) Chinese spring cv. Sumai 3, a well-known FHB resistant wheat cultivar, and Swedish spring wheat cv. SW Kadrilj which is susceptible to FHB were selected as contrasting plant materials for the experiments. Seeds of the cv. Sumai 3 were obtained from *SELGEN* (Stupice, Czech Republic), but seeds originated from *CIMMYT* (*Fusarium* head blight resistance screening nursery). Seeds of the cultivar SW Kadrilj were obtained from Central Institute for Supervising and Testing in Agriculture, Brno, Czech Republic. Seeds were sown on 4th April, 2016 in a greenhouse located at Crop Research Institute, Prague, Czech Republic (50°5′ N; 14°25′ E) under regulated watering till flowering stage. During flowering stage (9th June 2016; full flowering stage BBCH 65), plants of both cultivars were divided into three groups: control plants, plants inoculated with an inoculum of *Fusarium culmorum* strain B grown on potato dextrose agar (*Sigma-Aldrich*, St. Louis, USA) and plants treated with a solution of deoxynivalenol [DON; *Sigma-Aldrich*, 10 μg mm^{-3} diluted in phosphate buffer saline (PBS), pH 7.5, 0.05 % *Tween-20*; 10 mm^3 of DON solution was applied per one spike] using a single-floret method (Vančo *et al.* 2007; Chrpová *et al.* 2011). The spikes of all three plant groups were harvested for proteomic analysis at 10 dai and 10 d after DON application, respectively, when the plants were at early-dough stage (BBCH 73). The reason was to obtain samples affected by infection, but still not seriously damaged by a hemi-biotrophic pathogen; that is why young spikes still lacking apparent visual symptoms of infection were used for a proteomic analysis. The whole spikes including rachis and rachillas bearing developing grains coated by glumes, lemma and palea, but without awns, were taken for proteomic analyses. Following the samplings for proteomic analysis, visual evaluation of grain damage was carried out at 14 dai.

DON content was analysed in mature grains (BBCH 85) at 45 dai, *i.e.* at the end of plant growing season, using competitive enzyme-linked immunoassay *RIDASCREEN®FAST DON* (*RBiopharmAG*, Darmstadt, Germany). Four biological replicates of each sample were used for visual evaluation of grain damage and determination of DON content.

Proteomic analysis: Four biological replicates of frozen (-80 °C) spikes including rachis and rachillas bearing developing grains coated by glumes, lemma and palea, but without awns, were taken for proteomic analysis. Spikes were ground to a fine powder under liquid nitrogen using a mortar and pestle and total proteins were extracted using trichloroacetic acid (TCA)-phenol-acetone method as described by Wang *et al.* (2006). Finally, total proteins were precipitated by ammonium acetate, protein pelets were rinsed by acetone, dried, and dissolved in lysis buffer (*Bio-Rad* manual); pH of lysis buffer was adjusted to 8.5 by adding diluted NaOH and protein concentration was determined by *2D Quant* kit (*Bio-Rad*, Hercules, USA). Protein sample (30 µg) was used for sample labelling using CyDyes Fluorescent Dyes Cy3 or Cy5, and protein sample (15 µg) was added to an internal standard as a mixture of all samples used in the experiment and labelled with Cy2. Four biological replicates per each sample were employed in the analysis, two of which were labelled with Cy3 and the other two with Cy5. Protein minimal labelling by *CyDyes* was carried out according to the manual (*GE Healthcare*, Wauwatosa, Wisconsin, USA). After stopping the protein labelling reaction by adding excessive amount of lysine, rehydration buffer and 4.5 mm^3 of *Bio-Lyte* ampholyte were added to the mixed samples to the final volume of 455 mm^3. The samples were then loaded on isoelectric focusing (IEF) Cell tray using 24 cm linear immobilized pH gradient (IPG) strips (pI 5 - 8; *Bio-Rad*). The samples were subjected to a passive rehydration for 14 h followed by IEF using a rapid voltage slope till the final voltage of 10 000 V and the total of 75 000 Vh. After IEF, the strips with the samples were equilibrated using equilibration buffer I with dithiothreitol followed by equilibration buffer II with iodoacetamide according to the manual (*Bio-Rad*). The second dimension was carried out on 24 cm 12.5 % SDS-PAGE gels using *EttanDALTsix* (*Bio-Rad*). The *2D-DIGE* gels were scanned using *PharosFX* fluorescent imager (*Bio-Rad*) using three wavelengths at resolution of 600 dpi. Densitometric analysis of the *2D-DIGE* gel images was carried out using the software *PDQuest Advanced*, multichannel application, *v. 8.0.1* (*Bio-Rad*). Protein spot matching in the whole *2D-DIGE* image set was edited manually using *Group Consensus Tool*. Protein spot density in the individual samples was normalized at mean density of the corresponding spot in internal standard. Protein spots revealing significant quantitative (at least 2-fold change at 0.05 level determined by Student *t*-test) or qualitative (presence/absence) differences in nine biologically relevant ratios between the *cv*s. Sumai 3 control *vs.* Kadrilj control (SC/KC), Sumai 3 *Fusarium*-treated *vs.* Kadrilj *Fusarium*-treated plants (SF/KF), Sumai 3 DON-treated *vs.* Kadrilj DON-treated plants (SD/KD), Sumai 3 *Fusarium*-treated vs control plants (SF/SC), Sumai 3 DON-treated *vs.* control plants (SD/SC), Sumai 3 DON-treated *vs. Fusarium*-treated plants (SD/SF), Kadrilj *Fusarium*-treated *vs.* Kadrilj control plants (KF/KC), Kadrilj DON-treated *vs.* Kadrilj control plants (KD/KC), Kadrilj DON-treated *vs.* Kadrilj *Fusarium*-treated plants (KD/KF) were excised from preparative gels (1000 µg of protein load, proteins stained with Coomassie Brilliant Blue) using *ExQuest Spot Cutter* (*Bio-Rad*) and sent to protein identification by nanoLC-MS/MS.

Protein identification and bioinformatic analysis: Excised gel cubes were first destained with 1:1 mixture of acetonitrile and 0.1 M ammonium bicarbonate solution and then dried with acetonitrile. Solution of trypsin (12.5 ng mm^{-3}) was added to the cubes and the cubes were incubated for 25 min at 4 °C. Then excess of trypsin solution was removed and fresh solution of 50 mM ammonium bicarbonate was added. Digestion was carried out at 37 °C for 6 h. Afterwards trifluoroacetic acid was added to concentration of 0.5 % to stop digestion. In order to release peptides from gel cubes two rounds of sonication (15 min each) were performed: first in digestion buffer, which was replaced for second round with 50 % (v/v) acetonitrile solution in water. Both shares were combined and lyophilized.

Tandem mass spectra were acquired on *ESI-QToF* mass spectrometer *Maxis Impact* (*Bruker Daltonics*, Bremen, Germany) connected with nano liquid chromatograph *Dionex Ultimate3000 RSLC* nano (*Dionex*, Idstein, Germany). Peptides were dissolved in 20 mm^3 of the mixture of water:acetonitrile:formic acid (97:3:0.1) and 15 mm^3 were loaded onto trap column (*Acclaim PepMap 100 C18*, 100 µm × 2 cm). Bound peptides were washed for 5 min with solution containing 3 % of mobile phase B at flow rate of 5 mm^3 min^{-1}. Composition of mobile phases used during separation was as follows: mobile phase A water with 0.1 % (m/v) formic acid, mobile phase B acetonitrile with 0.1 % formic acid. Peptides were eluted to analytical column (*Acclaim PepMap RSLC C18* 75 µm × 150 mm, particle size 2 µm) using linear gradient of 3 to 35 % of mobile phase B in 30 min followed by column wash with 90 % of mobile phase B and reequilibration of the column for another injection with 3 % of B. Eluted peptides were introduced into *ESI* ionization source captive spray (*Bruker Daltonics*). Spray voltage was 1400 V, desolvation temperature 150 °C and flow of nitrogen 3 dm^3 min^{-1}. Precursors for fragmentation were selected in the range of 400 - 1 400 m/z. Up to five precursors could be selected for fragmentation from each mass spectrum. Fragmentation spectra were recorded in

the range of 50 - 2 200 m/z.

Peaklists were generated from raw data by *DataAnalysis 4.1* and uploaded to data management program *Proteinscape 3.1* (both *Bruker Daltonics*). *Mascot* searches were initialized from *Proteinscape* using following parameters: enzyme trypsin – 1 missed cleavage allowed, fixed modification – carbamidomethylation of cysteines, variable modification – oxidation of methionines, peptide tolerance 10 ppm in MS and 0.05 Da in MS/MS mode, respectively, custom made database containing proteomes of *Triticum aestivum* (130 673 sequences) and *Fusarium graminearum* (14 161 sequences). Sequences were downloaded from *Uniprot* website on the 4th of February 2019, furthermore sequences of common laboratory contaminants were added.

Two independent nanoLC-MS/MS analyses were carried out using two replicate preparative gels. Multiple proteins were identified in several spots. Therefore, the proteins identified in the given spot in both preparative gels or revealing the highest MS Score (when reliable identifications were obtained from only one of the two replicate gels) were considered for further interpretation. Application of these selection criteria led to matching of only one most reliable protein identification to each protein spot.

Theoretical pI and Mr values of each identified protein were calculated using the protein primary sequence from *Uniprot* database by *Compute pI/Mr* tool in *SwissProt* database (www.expasy.org). Protein domain analysis was carried out using *PFAM* database (www.pfam.sanger.uk), protein functional classification was carried out using *Gene Ontology* database (www.geneontology.org) using three main criteria: cellular localization, molecular function, and biological process. Enzyme numbers were assigned to proteins with an enzymatic activity using *BRENDA* database (www.brenda-enzymes.org).

Statistical analysis: Protein spots revealing differential relative abundance in at least one of the nine biologically relevant ratios were determined using Boolean analysis as an union of nine groups of protein spots fulfilling the two criteria: at least a 2-fold change in relative abundance at 0.05 level determined by Student *t*-test (*PDQuest Advanced, version*). For analysis of the individual protein spot relative abundances between the sample sets, two-way *ANOVA* analysis (genotype *vs*. treatment) was used followed by Duncan´s multiple range test at 0.05 using *STATISTICA* software, *v. 13* (*TIBCO*, Palo Alto, California, USA). Cluster analysis was applied for the analysis of the patterns of relative abundance changes in the whole set of 72 differentially abundant protein spots using Z-score transformed values of protein spot relative abundances, Euclidean distances, and Ward´s minimum criteria for cluster tree formation using *Permut Matrix*, *v. 1.9.3.* (Caraux and Pinloche 2005).

Results

Analysis of DON content in mature grains (45 days after *Fusarium* inoculation and DON application) revealed significant differences between the treatments (control *vs*. *Fusarium* inoculation *vs*. DON application) and between the wheat cultivars (Sumai 3 *vs*. SW Kadrilj). Resistant cv. Sumai 3 revealed significantly lower content of DON with respect to susceptible cultivar SW Kadrilj under the same treatments (Fig. 1) which is in accordance with the results published by Mesterházy *et al.* (2011).

The following experimental design was used for protein analysis: two wheat cultivars Sumai 3 and SW Kadrilj were exposed to three treatments: control, *Fusarium culmorum* inoculation, and DON application. Four biological replicates were taken from each sample, *i.e.*, a set of 24 2D-DIGE images corresponding to the individual samples plus 12 images corresponding to an internal standard (a mixed sample containing the same amounts of all the individual samples (μg) employed in the experiment) were subjected to densitometric analysis (Fig. 2*A,B*). Densitometric analysis of 2D-DIGE gels led to a selection of 72 reproducible protein spots matching to criteria on protein spot differential abundance, *i.e.,* a minimum of 2-fold change in protein spot relative abundance at 0.05 level determined by Student *t*-test in at least one of the following nine biologically relevant ratios: Sumai 3 control *vs. Fusarium* treatments, Sumai 3 control *vs.* DON treatments, Sumai 3 DON *vs. Fusarium* treatments; Kadrilj control *vs. Fusarium* treatments, Kadrilj control *vs.* DON treatments, Kadrilj DON *vs. Fusarium* treatments; control Sumai 3 *vs.* Kadrilj, *Fusarium* treatment Sumai 3 *vs.* Kadrilj, DON treatment Sumai 3 *vs.* Kadrilj (Fig. 2*A,B*; Table 1**)**. Relative abundance patterns of the 72 differentially abundant protein spots in the six experimental variants are shown in Fig. 2*B***.** The numbers of protein spots revealing differential relative abundance in at least one of the nine biologically relevant ratios are presented in Venn diagrams in Fig. 3. Evaluation of the patterns of relative abundance of 72 differentially abundant protein spots across all samples analyzed by cluster analysis revealed four distinct patterns of relative abundance within the set of two wheat cultivars and three treatments (Fig. 4).

Protein identification of 72 protein spots revealing differential abundance by LC-MS/MS approach revealed multiple protein identifications in most spots. However, based on a comparison of protein identification from two replicate preparation gels, proteins identified in both replicate gels and revealing highest MS score were selected as most reliable ones for the given protein spot. Thus, only one most reliable identification (*i.e*., identification determined in two replicate gels and revealing the highest MS score) was considered for further interpretation of protein spot potential biological function (Table 1). Out of 72 protein spots search against *Triticum aestivum* - *Giberella zeae* (*Fusarium*) database, 71 spots were assigned to wheat and one spot (6516) encoding actin was assigned to *Fusarium*. Functional categories of the identified protein spots according to biological process

Table 1. A list of identified proteins matched to 72 differentially abundant protein spots as determined by LC-MS/MS and the criteria explained in the text. Score means *MASCOT Score*. pI/Mr theor. means pI and Mr values calculated from identified protein sequence using pI/Mr tool in *SwissProt* database while pI/Mr exp. means pI and Mr values determined from protein spot position in 2D-DIGE gel. Proteins followed by an *asterisk* were identified by *BLASTP* search against *Uniprot* database (www.uniprot.org), taxonomy *Triticum aestivum*, in February 2019.

SSP	Accession number	Protein name	Score	Ident [%]	Number of unique peptides	pI/Mr theor. pI/Mr exp.	Cluster
Amino acid metabolism							
112	A0A3B6B7M3	Glutamine synthetase OS=*Triticum aestivum* OX=4565 PE=3 SV=1*	651	100	4	5.89 / 46.09 5.25 / 50.37	2
204	A0A3B6B7M3	Glutamine synthetase OS=*Triticum aestivum* OX=4565 PE=3 SV=1	64		3	5.72 / 45.09 5.18 / 50.93	2
1104	A0A3B6HPD4	Glutamine synthetase OS=*Triticum aestivum* OX=4565 PE=3 SV=1	702		8	5.45 / 38.68 5.34 / 45.30	3
2308	A0A3B6PIZ5	3-isopropylmalate dehydratase large subunit, chloroplastic*	270	98	3	6.30 / 54.84 5.59 / 57.09	4
4406	A0A3B6LDV5	5-methyltetrahydropteroyltriglutamate--homocysteine methyltransferase 1-like*	949	99	16	5.86 / 85.45 5.94 / 81.33	3
4506	A0A3B6K9Q1	5-methyltetrahydropteroyltriglutamate--homocysteine methyltransferase 1-like*	72	100	3	6.02 / 89.24 5.96 / 82.27	3
5502	A0A3B6K9Q1	5-methyltetrahydropteroyltriglutamate--homocysteine methyltransferase 1-like*	760	100	8	6.02 / 89.24 6.00 / 82.11	3
5510	A0A3B6K9Q1	5-methyltetrahydropteroyltriglutamate--homocysteine methyltransferase 1-like*	193	100	4	6.02 / 89.24 6.10 / 88.02	4
6501	A0A3B6JCF8	5-methyltetrahydropteroyltriglutamate--homocysteine methyltransferase 1-like*	748	99	9	7.02 / 91.27 6.15 / 88.09	4
6601	A0A3B6HXB3	5-methyltetrahydropteroyltriglutamate--homocysteine methyltransferase 1-like*	129	99	4	5.89 / 84.43 6.23 / 88.01	1
5210	A0A3B6NVU6	Aspartate aminotransferase OS=*Triticum aestivum* OX=4565 PE=4 SV=1	479		9	6.77 / 51.97 6.03 / 49.76	2
7303	A0A3B5Y096	Serine hydroxymethyltransferase OS=*Triticum aestivum* OX=4565 PE=3 SV=1	260	100	4	8.31 / 58.10 6.63 / 58.39	2
7307	A0A3B6C5R2	glutamate--glyoxylate aminotransferase 2 isoform X1*	757	99	23	6.57 / 53.31 6.67 / 56.35	1
ATP metabolism							
309	A0A3B5Y5K9	ATP synthase subunit beta OS=*Triticum aestivum* OX=4565 PE=3 SV=1	663		5	5.72 / 59.16 5.23 / 58.8	4
1206	A0A3B6EIN4	ATP synthase subunit beta OS=*Triticum aestivum* OX=4565 PE=3 SV=1	2512		14	5.85 / 58.93 5.44 / 57.92	3
4306	P12112	ATP synthase subunit alpha, chloroplastic OS=*Triticum aestivum* OX=4565 GN=atpA PE=3 SV=2	981		9	6.11 / 55.29 5.96 / 65.66	1
2304	A0A3B6RD12	ATP synthase subunit alpha OS=*Triticum aestivum* OX=4565 PE=3 SV=1	1357		8	6.43 / 55.36 5.6 / 63.77	4
4510	A0A3B5Y5K9	ATP synthase subunit beta OS=*Triticum aestivum* OX=4565 PE=3 SV=1	55		3	5.72 / 59.16 5.9 / 77.19	1
1409	A0A341Y4U2	V-type proton ATPase catalytic subunit A*	835	100	19	5.19 / 67.79 5.36 / 72.79	1
Carbohydrate metabolism							
108	A0A3B6NSF0	Phosphoribulokinase OS=*Triticum aestivum* OX=4565 PE=3 SV=1	1536		10	5.72 / 45.09 5.16 / 47.87	1
111	A0A3B6NSF0	Phosphoribulokinase OS=*Triticum aestivum* OX=4565 PE=3 SV=1	1120		11	5.72 / 45.09 5.22 / 47.85	2
3203	A0A3B6NSF0	Phosphoribulokinase OS=*Triticum aestivum* OX=4565 PE=3 SV=1	577		6	5.72 / 45.09 5.73 / 51.98	1
1107	A0A3B5ZZM6	Phosphoglycerate kinase OS=*Triticum aestivum* OX=4565 PE=3 SV=1	1576		17	6.99 / 49.75 5.4/48.92	2

1213	A0A3B5ZZM6	Phosphoglycerate kinase OS=*Triticum aestivum* OX=4565 PE=3 SV=1	2341		16	6.99 / 49.75 5.33/49.5	1
1202	A0A1D6S518	UTP-glucose-1-phosphate uridylyltransferase OS=*Triticum aestivum* OX=4565 PE=3 SV=1	384		8	5.20 / 51.66 5.34/58.08	4
1306	A0A2X0TUH3	Beta-amylase OS=*Triticum aestivum* OX=4565 GN=CAMPLR22A2D_LOCUS2061 PE=3 SV=1	87		2	5.41 / 57.05 5.36/61.05	4
1309	P93594	Beta-amylase OS=*Triticum aestivum* OX=4565 GN=BMY1 PE=2 SV=1	683		11	5.24 / 56.6 5.41/60.26	3
1311	A0A3B6H0L0	2,3-bisphosphoglycerate-independent phosphoglycerate mutase*	1915	100	19	5.48 / 60.71 5.48/68.89	1
2403	A0A3B6TID0	transketolase, chloroplastic*	529	99	20	5.88 / 80.06 5.51/78.28	3
3404	A0A1D6D1Q3	Pyrophosphate--fructose 6-phosphate 1-phosphotransferase subunit beta OS=*Triticum aestivum* OX=4565 GN=PFP-BETA PE=3 SV=1	234		2	5.83 / 60.56 5.77/70.75	4
4103	A0A3B6SGH3	Fructose-bisphosphate aldolase OS=*Triticum aestivum* OX=4565 PE=3 SV=1	126		4	6.38 / 37.88 5.9/47	3
4505	A0A3B6SD29	Sucrose synthase OS=*Triticum aestivum* OX=4565 PE=3 SV=1	185		3	5.76 / 92.34 5.91/86.89	1
7102	A0A3B6RKE1	Glyceraldehyde-3-phosphate dehydrogenase OS=*Triticum aestivum* OX=4565 PE=3 SV=1	403		7	6.40 / 36.21 6.52/45.41	3
7105	A0A3B6NQQ5	Glyceraldehyde-3-phosphate dehydrogenase OS=*Triticum aestivum* OX=4565 PE=3 SV=1	1438		16	7.05 / 36.59 6.82/42.87	4
Cytoskeleton							
1105	A0A1D6DJ20	actin-1-like*	2638	100	13	5.37 / 41.79 5.35 / 49.52	4
2101	A0A3B6KDW0	Actin-3*	2692	100	17	5.32 / 45.14 5.5 / 48.32	3
3304	A0A1D5X5C6	actin-3*	41	100	2	5.31 / 41.62 5.73 / 63.25	4
Organism: *Fusarium* (*Gibberella zeae*)							
6516	I1RT41	Actin, partial*	18	100	2	5.45 / 41.6 6.39 / 90.76	3
Lipid metabolism							
6506	A0A3B6MY02	Lipoxygenase OS=*Triticum aestivum* OX=4565 PE=3 SV=1	145		5	6.17 / 96.56 6.22 / 97.2	3
Photoreceptor							
2204	A0A3B6DE51	ultraviolet-B receptor UVR8-like*	1672	100	13	5.42 / 46.85 5.55/53.59	3
Photosynthesis							
12	A0A1D5ZLT0	Chlorophyll *a-b* binding protein, chloroplastic OS=*Triticum aestivum* OX=4565 PE=3 SV=1	109		2	5.29 / 28 5.08/31.74	
1008	A0A3B6PLM0	Chlorophyll *a-b* binding protein, chloroplastic OS=*Triticum aestivum* OX=4565 PE=3 SV=1	470		6	8.69 / 29.29 5.45/30.24	2
2007	A0A1D5RS51	Chlorophyll *a-b* binding protein, chloroplastic OS=*Triticum aestivum* OX=4565 PE=3 SV=1	336		4	5.14 / 28.2 5.63/19.68	2
1110	A0A3B6HWM5	Ribulose bisphosphate carboxylase/oxygenase activase A, chloroplastic*	639	100	7	6.91 / 50.93 5.43/46.52	2
3205	A0A3B6JII7	Ribulose bisphosphate carboxylase/oxygenase activase A, chloroplastic isoform X2*	1381	95	9	8.62 / 45 5.77/57.54	
4109	A0A3B6HWM5	Ribulose bisphosphate carboxylase/oxygenase activase A, chloroplastic*	874	100	8	6.91 / 50.93 5.86/47.11	2
4004	A0A077RST2	Carbonic anhydrase OS=*Triticum aestivum* OX=4565 GN=TRAES_3BF026200060CFD_c1 PE=3 SV=1	868		7	8.35 / 27.96 5.98/30.38	1
5007	A0A077RST2	Carbonic anhydrase OS=*Triticum aestivum* OX=4565 GN=TRAES_3BF026200060CFD_c1 PE=3 SV=1	158		2	8.35 / 27.96 6.07/29.62	1
5604	P11383	Ribulose bisphosphate carboxylase large chain OS=*Triticum aestivum* OX=4565 GN=rbcL PE=1 SV=2	415		16	6.22 / 52.85 6.04/85.98	3

6310	P11383	Ribulose bisphosphate carboxylase large chain OS=*Triticum aestivum* OX=4565 GN=rbcL PE=1 SV=2	201		2	6.22 / 52.85 6.2/55.9	4
7305	P11383	Ribulose bisphosphate carboxylase large chain OS=*Triticum aestivum* OX=4565 GN=rbcL PE=1 SV=2	207		5	6.22 / 52.85 6.32/59.9	1
Protein folding							
306	A0A3B6RB14	RuBisCO large subunit-binding protein subunit beta, chloroplastic*	2684	99	18	5.56 / 63.94 5.2/69.06	4
408	A0A3B6I2A6	RuBisCO large subunit-binding protein subunit beta, chloroplastic*	1185	97	11	5.92 / 62.33 5.12 / 69.95	4
410	A0A3B6RB14	RuBisCO large subunit-binding protein subunit beta, chloroplastic*	565	99	22	5.56 / 63.94 5.14 / 69.54	4
418	A0A3B6I2A6	RuBisCO large subunit-binding protein subunit beta, chloroplastic*	790	97	9	5.92 / 62.34 5.13 / 66.63	2
416	A0A3B6C9B5	heat shock cognate 70 kDa protein 2-like*	129	99	6	5.07 / 71.14 5.27/75.2	4
1408	A0A3B5Z104	heat shock cognate 70 kDa protein 2-like*	1144	100	12	5.13 / 71.02 5.36/75.25	3
Protein metabolism (translation)							
5513	A0A3B6TJ13	glycine--tRNA ligase, mitochondrial 1-like*	306	100	7	6.71 / 82.04 5.96/77.81	1
7214	A0A3B6RM24	Elongation factor 1-gamma 2*	795	100	10	6.18 / 46.8 6.31/51.57	1
Redox metabolism							
1203	A0A3B6ILN0	monodehydroascorbate reductase-like*	442	97	9	5.23 / 46.37 5.38/51.86	3
4011	A0A3B6HQ83	L-ascorbate peroxidase 1, cytosolic*	1126	99	15	5.85 / 27.48 5.92/31.29	4
6305	A0A3B5XW54	Dihydrolipoyl dehydrogenase OS=*Triticum aestivum* OX=4565 PE=3 SV=1	191		13	6.72 / 52.74 6.32/62.51	2
8512	A0A3B6PHD6	Catalase OS=*Triticum aestivum* OX=4565 PE=3 SV=1	223		9	6.70 / 56.89 7.01/65.47	2
Respiration							
8514	A0A3B6EF27	ATP-citrate synthase beta chain protein 1*	249	99	8	7.17 / 65.96 7.19/69.39	3
5501	A0A3B6KT79	Aconitate hydratase OS=*Triticum aestivum* OX=4565 PE=3 SV=1	351		9	6.63 / 10.69 6/96.01	3
4003	A0A3B5XY18	Malate dehydrogenase OS=*Triticum aestivum* OX=4565 PE=3 SV=1	1245		7	5.92 / 35.07 5.92/42.29	1
4402	A0A3B6HYA0	NADH dehydrogenase [ubiquinone] iron-sulfur protein 1, mitochondrial*	814	99	16	6.38 / 80.23 5.86/81.73	1
Secondary metabolism							
3301	A0A3B5Y4U7	BAHD acyltransferase DCR*	546	98	4	5.41 / 47.6 5.67/64.1	4
5611	A0A3B6PL15	Phenylalanine ammonia-lyase OS=*Triticum aestivum* OX=4565 PE=3 SV=1	130		6	5.82 / 75.61 6.04/77.28	3
Stress and defense							
6002	A0A3B6EIU5	glutathione S-transferase 1-like*	672	98	3	5.78 / 23.27 6.41 / 19.02	3
7009	A0A3B6C021	ricin B-like lectin R40G2*	2043	99	12	6.52 / 38.82 6.8 / 40.22	1
7111	A0A3B6C021	ricin B-like lectin R40G2*	947	99	10	6.52 / 38.82 6.75 / 40.94	1

criterion when only one most reliable protein identification was considered are given in Fig. 5. The most numerous protein functional categories represent carbohydrate metabolism (15 spots), amino acid metabolism (13 spots), and photosynthesis (11 spots) while the remaining ten categories were assigned to less than 10 spots.

Discussion

The present study aimed to investigate proteomic response to *F. culmorum* inoculation and deoxynivalenol (DON) application in spikes of two wheat cultivars with contrasting resistance to FHB, Sumai 3, known as a resistance source, and SW Kadrilj, a susceptible cultivar to FHB. We wanted to study plant acclimation response to the fungus and its mycotoxin. So we took the samples for proteomic analysis at 10 dai.

Ding *et al.* (2017) studied proteome response in Sumai 3 and susceptible wheat cv. Huaimai 27 only 24 h following *F. graminearum* inoculation and thus identified several signalling proteins revealing differential abundance indicating an alarm phase of plant stress response. In our study, protein identifications obtained from wheat spikes at 10 dai reveal an acclimation response of the plants as indicated by profound alterations in cellular metabolism, namely energy metabolism including photosynthesis and ATP metabolism, carbohydrate metabolism, amino acid metabolism and associated nitrogen metabolism as well as secondary metabolism indicating biosynthesis of novel compounds with protective properties. Moreover, relatively few but important identifications belonging to stress-protective proteins („protein folding," „redox metabolism" and „stress and defence" categories) were also obtained in *Fusarium*- and DON-treated plants. A scheme summarising major protein functional categories affected by *Fusarium*- or DON treatments is given in Fig. 6.

Photosynthesis, ATP metabolism, carbohydrate metabolism: Generally, based on the experimental data, it can be concluded that anabolic processes, namely photosynthesis and ATP biosynthesis, are downregulated in *Fusarium*-treated or DON-treated plants with respect to untreated ones (control) in both wheat cultivars although genotypic differences can be observed between Sumai 3 and SW Kadrilj.

For example, regarding RubisCO LSU, an increase in RubisCO LSU (spots 5604, 6310) in *Fusarium*-treated plants with respect to untreated ones was found in Sumai 3. Alterations in photosynthesis-related proteins included both proteins associated with plant photosystems on thylakoid membranes (so-called primary or light reactions) as well as stromal proteins associated with carbon assimilation (RubisCO and Calvin cycle enzymes). A decrease in chlorophyll *a/b* binding proteins (spots 12, 1008, 2007) as a crucial component of antenna complexes (LHC) of both photosystems (PS I and PS II) was found in DON-treated plants with respect to control indicating a downregulation of photosynthesis. In contrast, an increase in RubisCO LSU (spots 5604, 6310) in *Fusarium*-treated plants with respect to untreated ones was found in Sumai 3 which may indicate its resistance to *Fusarium* infection and mobilization of carbon assimilation in Sumai 3 since carbon assimilation is necessary for further biosynthetic reactions such as biosynthesis of protective phenolic compounds (see data on secondary metabolism).

RubisCO activase (RCA) is involved in a release of inhibitory sugar phosphates such as ribulose-1,5-bisphosphate, a RubisCo substrate, from an active site of RubisCO. RCA thus allows CO_2 binding and carbamoylation of the RubisCO active site. Carbonic anhydrase (CA) catalyzes a reversible interconversion between carbon dioxide and hydrogencarbonate thus providing carbon dioxide to RubisCO active site. However, decreased content of crucial enzymes supporting RubisCO carboxylation activity such as RubisCO activase (spots 1110, 4109) and carbonic anhydrase (spots 4004, 5007) in *Fusarium*-inoculated and DON-treated plants with respect to control indicate a downregulation of RubisCO carboxylation activity. In contrast, enhanced levels of RubisCO chaperones such as CPN60β (spots 306, 408) in *Fusarium*-treated plants with respect to control in SW Kadrilj indicate an enhanced need to protect RubisCO conformation and enzymatic activity in the susceptible wheat cultivar when exposed to *Fusarium* infection. Consistently with declined content of enzymes (CA, RCA) involved in RubisCO activation, decreased levels of phosphoribulokinase (PRK; spots 108, 111, 3203) were found in *Fusarium*-treated plants with respect to control. PRK is a crucial enzyme of Calvin cycle involved in regeneration of RubisCO substrate ribulose-1,5-bisphosphate from ribulose-5-phosphate. Consistently with decreased content of the proteins associated with carbon assimilation, decreased content of α and β subunits of chloroplastic ATP synthase (spots 309, 2304, 4306, 4510) were found in *Fusarium*- and DON-treated plants

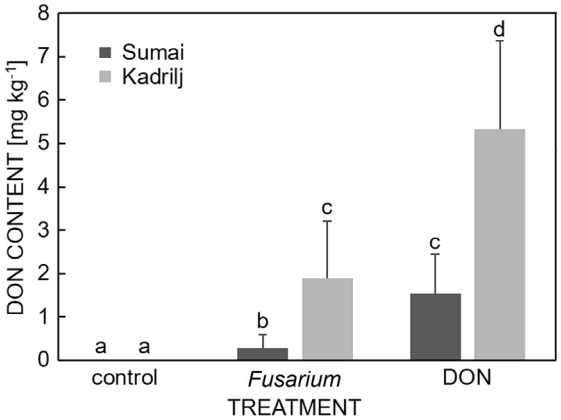

Fig. 1. The content of DON in mature grains of FHB resistant wheat cultivar Sumai 3 (*black columns*) and FHB susceptible wheat cultivar SW Kadrilj (*gray columns*) in plants grown under control conditions, *Fusarium culmorum* inoculation and DON application at 45 dai. Means ± SDs, $n = 6$. Different letters indicate significant differences determined by two-way *ANOVA* followed by Duncan´s multiple range test (DMRT) at 0.05 level.

with respect to control ones. Similarly to our results, decreased levels of photosynthesis-related proteins were also found by Ding *et al.* (2011, 2017).

Consistently to alterations in photosynthesis, alterations in carbohydrate metabolism were found in *Fusarium*-infected or DON-treated plants. Regarding carbohydrate catabolism, enhanced levels of glycolysis enzymes including fructose-bisphosphate aldolase (FBP ALDO; spot 4103), glyceraldehyde-3-phosphate dehydrogenase (GAPDH; spots 7102, 7105), phosphoglycerate kinase (PGK; spots 1107, 1213), and 2,3-bisphosphoglycerate independent phosphoglycerate mutase (PGM; spot 1311) were found in *Fusarium*- and DON-treated Sumai 3 with respect to control as well as with respect to susceptible Kadrilj plants. Enhanced levels of glycolysis enzymes in *Fusarium*- and DON-treated Sumai plants indicate an enhanced need for energy during an active plant response to pathogen. However, regarding catabolic reactions aimed at hydrolysis of storage carbohydrates such as starch, Sumai 3 revealed lower content of beta-amylase (spots 1306, 1309) with respect to susceptible Kadrilj in DON-treated plants. This finding indicates that Sumai was able to acquire sufficient energy resources by photosynthesis and intermediate metabolism and does not need to degrade storage molecules.

Moreover, enhanced content of sucrose synthase (SuSy; spot 4505) and UTP-glucose-1-phosphate uridylyltransferase also known as UDP-glucose pyrophosphorylase (UGPase; spot 1202) which can act as anabolic enzymes due to production of activated UDP-glucose were found in *Fusarium*-treated Sumai with respect to Kadrilj plants. This finding indicates enhanced biosynthesis of novel sugar-containing compounds (*e.g.*, glycoproteins, glycolipids, etc.) which may play an important role in plant response to pathogen in resistant Sumai. For example, lectins can be given as glycoproteins

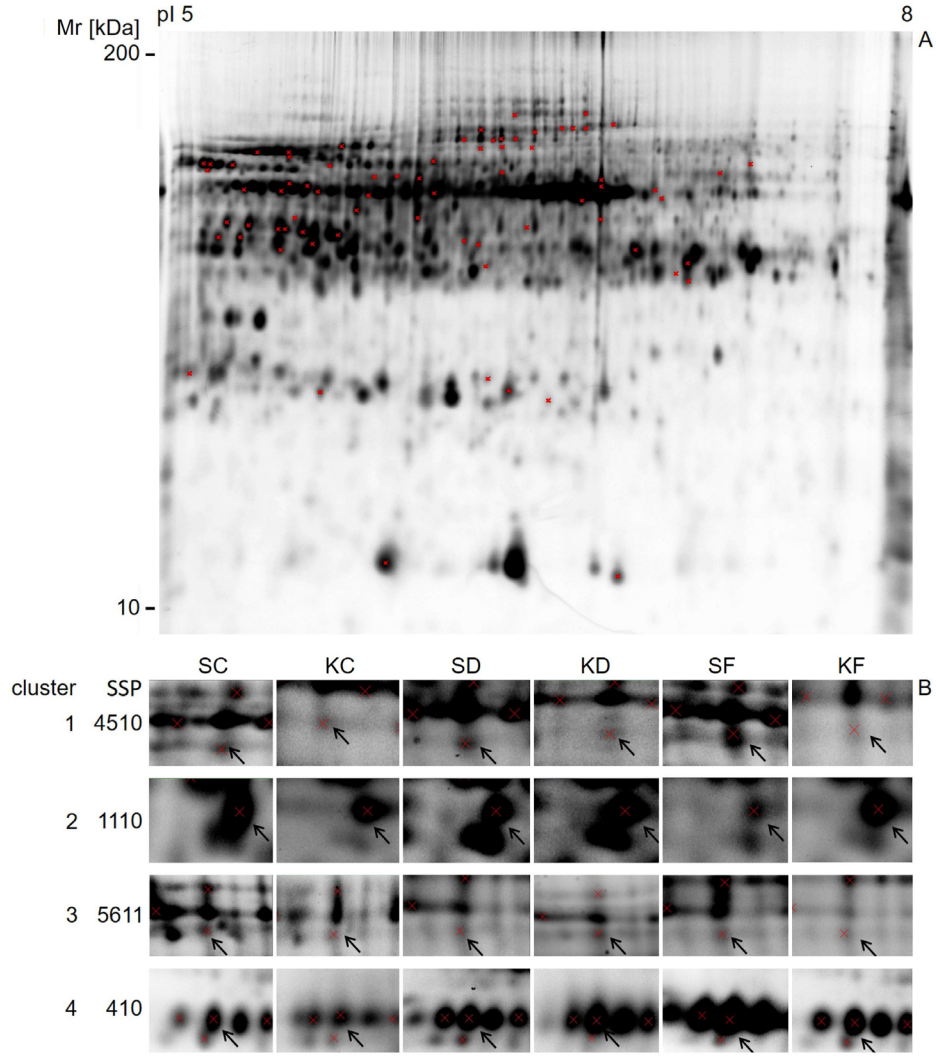

Fig. 2. A representative 2D-DIGE gel image of an internal standard with indicated positions of 72 differentially abundant protein spots (*A*) and detailed views on the dynamics of protein spot relative abundance in four representative differentially abundant protein spots (ssp 410, 1110, 4510, 5611) belonging to different clusters of protein spot abundance patterns. (*B*) *Arrows* indicate the positions of the representative protein spots. KC - SW Kadrilj control plants; KD - SW Kadrilj DON-treated plants; KF - SW Kadrilj *Fusarium*-treated plants; SC - Sumai 3 control plants; SD - Sumai 3 DON-treated plants; SF - Sumai 3 *Fusarium*-treated plants.

involved in plant defense against pathogens (reviewed in Lannoo and Van Damme 2014). In addition, UDP-glucose is also a monomer for cellulose biosynthesis indicating cell wall remodelling in *Fusarium*-treated Sumai which corresponds with alterations in enzymes of phenylpropanoid pathway involved in biosynthesis of lignin monomers. Moreover, it recently becomes evident that UDP-glucose does not only act as a substrate for oligosaccharide and polysaccharide biosynthesis but it is also involved in stress-related signalling pathways. In animals, UDP-glucose acts as an extracellular signaling molecule via interaction with G-protein coupled receptors (Chambers *et al.* 2000). In plants, recent studies indicate an association of UDP-glucose with enhanced biomass accumulation; however, excess UDP-glucose levels were associated with programmed cell death (PCD; Chivasa *et al.* 2013) indicating a potential role of UDP-glucose in plant stress signaling (Janse van Rensburg and Van den Ende 2018). Moreover, in *Fusarium*-infected plants, UDP-glucose serves as a substrate for DON detoxification to DON-3-O-glucoside which is catalyzed by grain uridine diphosphate glucosyltransferase. Enhanced content of UDP-glucose producing enzymes in Sumai 3 with respect to Kadrilj correlates with significantly reduced DON content in the FHB-resistant wheat genotype. An enzyme with UDP-glucosyltransferase activity was proposed to be encoded by *Fhb1* locus associated with superior FHB resistance in Sumai 3 (Lemmens *et al.* 2005).

Lipid metabolism: Lipoxygenase (LOX) is involved in hydroperoxidation of polyunsaturated fatty acids in membrane lipids such as linolenic acid leading to formation of oxylipins and other metabolites such as jasmonic acid (JA) involved in plant-pathogen signaling (reviewed by Wasternack and Hause 2013). Enhanced content of LOX (ssp 6506) in Sumai with respect to Kadrilj plants under control conditions may indicate an enhanced pathway leading to JA biosynthesis. Besides, LOX produced hydroperoxides of unsaturated fatty acids lead to production of ROS which reveal damage to plant membrane but can also have a signalling function; a close relationship was proposed for LOX and ROS (Siedow 1991, Glickman and Klinman 1996, Maalekuu *et al.* 2006). Thus, enhanced LOX (ssp 6506) in Sumai *vs.* Kadrilj plants may indicate enhanced LOX-induced and ROS-madiated signalling in Sumai.

Redox metabolism: Plant response to pathogen attack leads to enhanced levels of ROS some of which, *e.g.*, hydrogen peroxide, can act as signaling molecules. However, enhanced ROS levels lead to damage of biomolecules thus plants activate ROS scavenging enzymes to reduce enhanced ROS levels. Alterations in H_2O_2 decomposing enzymes monodehydroascorbate reductase (MDAR; spot 1203) ascorbate peroxidase (APX; spot 4011), and catalase (CAT; spot 8512) were found indicating enhanced H_2O_2 levels and thus an enhanced need to decompose them.

Secondary metabolism: Alterations in key enzymes of phenylpropanoid pathway leading to biosynthesis of phenolic compounds including flavonoids, anthocyanins, lignin monomers, etc., *i.e.*, molecules with protective function in response to pathogens, were found. Phenylalanine ammonia lyase (PAL) catalyses conversion of L-phenylalanine to ammonia and *trans*-cinnamic acid which represents the first step in the biosynthesis of a wide array of phenolic compounds including salicylic acid (SA) involved in plant signalling in response to pathogens. PAL reveals enhanced content in *Fusarium*-treated Sumai with respect to DON-treated Sumai plants.

BAHD acyltransferases use acyl-CoA thioesters as donors of acyl group in an acylation step in the biosynthesis of a wide array of phenolic compounds (reviewed in Bontpart *et al.* 2015). BAHD acyltransferase DCR was increased in *Fusarium*-treated Sumai in comparison to control plants as well as *Fusarium*-treated Kadrilj plants. This indicates an enhanced biosynthesis of phenolics in *Fusarium*-treated Sumai indicating one of the molecular mechanisms underlying its superior *Fusarium* resistance. BAHD acyltransferases act as monomeric enzymes and

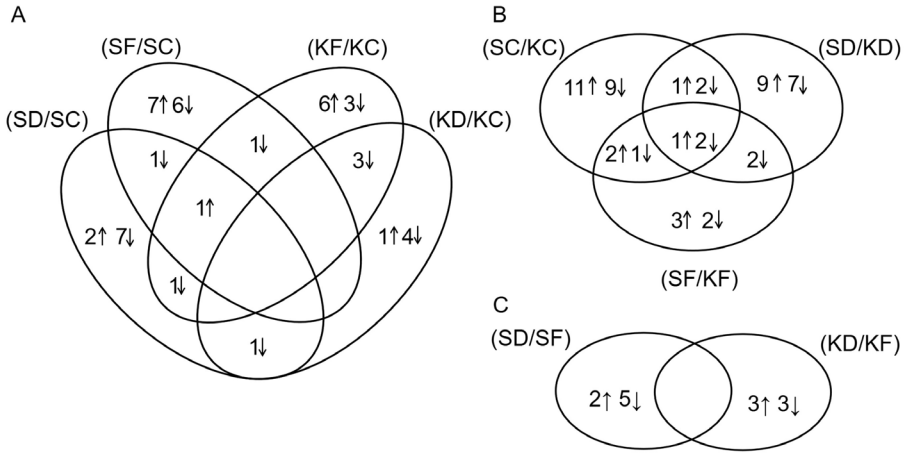

Fig. 3. Venn diagrams showing the numbers of differentially abundant protein spots revealing a significant increase (↑) or a decrease (↓) in relative abundance between *Fusarium*- or DON-treated plants with respect to control (*A*), between Sumai 3 *vs.* SW Kadrilj cultivars (*B*), and between DON *vs. Fusarium* treatments (*C*). See Fig. 2 for abbreviations.

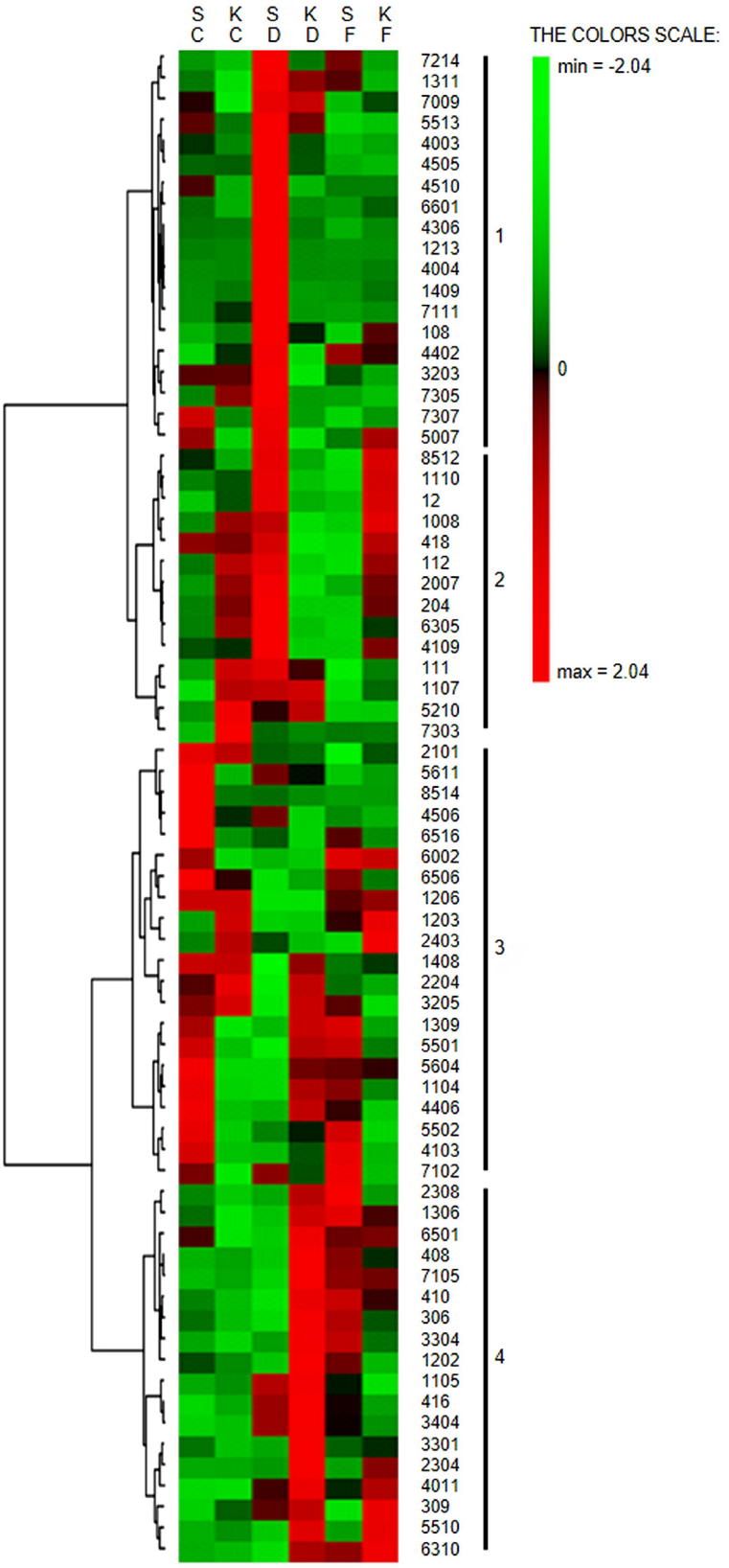

Fig. 4. Cluster analysis of 72 differentially abundant protein spots excised for protein identification. Z-score transformed data on protein relative abundance, Euclidean distances and Ward´s minimum criteria were used for construction of the cluster using *Permut Matrix* software, *v. 1.9.3* (Caraux and Pinloche 2005). The numbers 1 to 4 indicate the different clusters encompassing different patterns of protein spot relative abundances across the given sample set.

reveal a wide genetic diversity in their structure and a spectrum of substrates. Acylation of some phenolic compounds affects their involvement in plant defense mechanisms against pathogens; *e.g.*, acylation of avenacins enhanced their involvement in pathogen defense in oats (Mugford *et al.* 2009).

It is interesting that both PAL (ssp 5611) and BAHD acyltransferase DCR (ssp 3301) revealed enhanced content in *Fusarium*-treated variants of Sumai 3 in comparison to DON-treated variants. This finding may indicate stronger response of the plant to fungal pathogen than to the sole mycotoxin and could be associated with an enhanced biosynthesis of lignin components in infected plant cells in order to prevent pathogen spread. Recent studies indicate an important role of plant cell wall composition in mediating FHB resistance (Lionetti *et al.* 2015). Similarly, Gunnaiah *et al.* (2012) in their metabolo-proteomic study on resistant wheat cv. Nyubai concluded that FHB resistance in this cultivar is associated with cell wall thickening due to enhanced levels of enzymes involved in phenylpropanoid biosynthesis resulting in deposition of hydroxycinnamic acid amides, phenolic glucosides and flavonoids. Based on our results, it can be concluded that enhanced abundances of enzymes involved in biosynthesis of phenolic compounds represent an exclusive plant response to the *Fusarium* pathogen but not to sole mycotoxin (DON) application. The major reason of these differences may lie in the fact that enhanced content of phenolic compounds including both protective compounds and cell wall components are efficient for plant defense against pathogen attack but could not contribute to mycotoxin detoxification.

Protein folding, stress- and defence-related proteins: RubisCO chaperones, namely CPN60β (ssp 306, 408, 410, 418) revealed enhanced content in *Fusarium*-treated Kadrilj plants with respect to control ones indicating an enhanced need for RubisCO protection in *Fusarium*-treated spikes of susceptible Kadrilj cultivar. Similarly, enhanced content of two isoforms Hsc70 2-like protein (ssp 416, 1408) were found in both *Fusarium*-treated Sumai and Kadrilj plants with respect to control indicating enhanced response to pathogen infection since Hsc70 is known to function as a cochaperone interacting with SGT1 protein *via* evolutionarily conserved SGS domain in SGT1. In *A. thaliana*, four Hsc70 isoforms were identified, out of them Hsc70-1 and Hsc70-3 isoforms are constitutitvely expressed in plant cell cytoplasm while Hsc70-2 and Hsc70-4 isoforms are pathogen-inducible. Hsc70-SGT1 complex is known to play an important role in resistance gene (*R* gene) triggered plant immunity (Noël *et al.* 2007). We have identified enhanced levels of SGT1 protein in *Fusarium*-treated barley cultivars in our previous study (Kosová *et al.* 2017).

Glutathione-S-transferases (GST) represent a large family of enzymes using glutathione conjugation to xenobiotics as the first step to their degradation. GST reveals a decreased content in DON-treated Sumai in comparison to *Fusarium*-treated Sumai as well as DON-treated Kadrilj indicating enhanced resistance of DON-treated Sumai.

Ricin B lectins are glycoproteins involved in saccharide signaling and response to plant pathogens. Enhanced level of ricin B lectin was found in DON-treated Kadrilj with respect to Sumai as well as in *Fusarium*-treated Kadrilj plants with respect to DON-treated ones. Ricin B lectins were reported in plant response to pathogens and were found to be involved in caspase 3-like protease-induced apoptosis (Shahidi-Noghabi *et al.* 2008, reviewed in Lannoo and Van Damme 2014)., Recently, a chimeric lectin with two agglutinin domains and a pore-forming toxin-like domain was mapped as a candidate gene to FHB1, the major FHB resistance-associated QTL on 3BS conferring FHB resistance in Sumai 3 (Rawat *et al.* 2016).

Amino acid metabolism and nitrogen metabolism: Glutamine synthetase (GS) represents a crucial enzyme in nitrogen metabolism since it is involved in ammonia assimilation *via* its ligation to glutamate resulting in

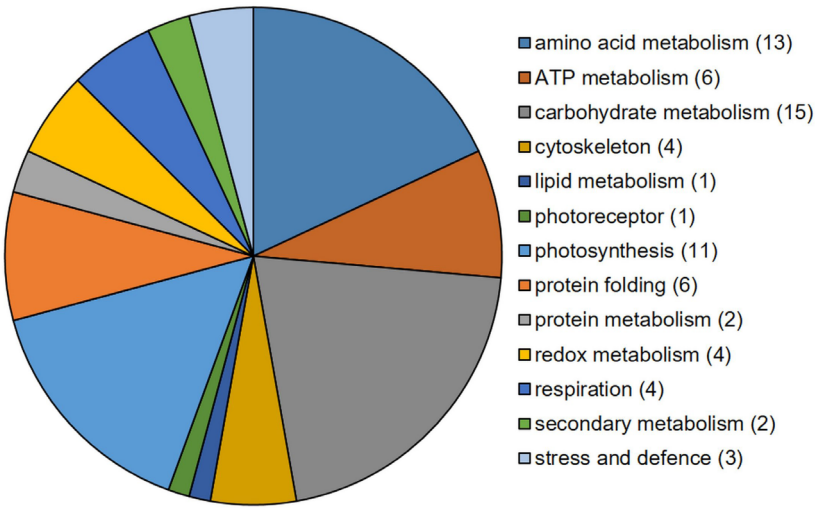

Fig. 5. Functional classification of the 72 identified protein spots based on biological process criterion. Numbers in brackets following each protein functional category indicate a number of proteins assigned to this category.

glutamine formation. Decreased GS content (spot 112, 204) was found in Sumai with respect to Kadrilj under various treatments (control, DON-treated and *Fusarium*-treated plants) indicating enhanced need for ammonia assimilation in Kadrilj. Similarly, Sumai 3 also revealed lower content of aminotransferases enzymes, namely aspartate aminotransferase (spot 5210) and glutamate-glyoxylate aminotransferase 2 isoform X1 (spot 7307), which are involved in reversible interconversions between amino acids and oxoacids. Decreased content of GS and aminotransferases in Sumai 3 may indicate a lower rate of nitrogen assimilation and transfer in DON-treated Sumai with respect to DON-treated Kadrilj as well as control Sumai plants.

Isopropylmalate dehydratase (ssp 2308) was found increased in DON-treated Sumai plants in comparison to control Sumai and susceptible Kadrilj plants. A similar enzyme of isopropylmalate dehydrogenase is known to be involved in leucine and other branched amino acids biosynthesis as well as in glucosinolate biosynthesis in *A. thaliana*. These data indicate an important role of isopropylmalate dehydratase in plant protection against pathogens and herbivores (He *et al.* 2009); however, cereals do not accumulate glucosinolates.

Several protein spots (spots 4406, 4506, 5502, 5510, 6501, 6601) were identified as 5-methyltetrahydropteroyltriglutamate homocysteine methyltransferase 1-like. This enzyme is involved in methionine biosynthesis by catalyzing a transfer of a methyl group from 5-methyltetrahydrofolate to homocysteine resulting in methionine formation. The spots revealed mixed patterns of relative abundances with higher content in Sumai with respect to Kadrilj as well as increased levels in *Fusarium*-treated plants with respect to DON-treated ones. An enhanced biosynthesis of methionine may contribute to enhanced stress response in resistant Sumai since methionine represents a precursor of S-adenosylmethionine which is an universal methylation agent in plant cells and whose enhanced levels were reported in several stress-treated plants (reviewed in Kosová *et al.* 2018).

Cytoskeleton: Three protein spots (ssp 1105, 2101 and 3304) were assigned as wheat actin isoforms and one protein spot (ssp 6516) was identified as actin of *Fusarium* origin. While actin of *Fusarium* origin revealed an increase in *Fusarium*-treated Sumai plants with respect to control the actin isoforms of wheat origin revealed a

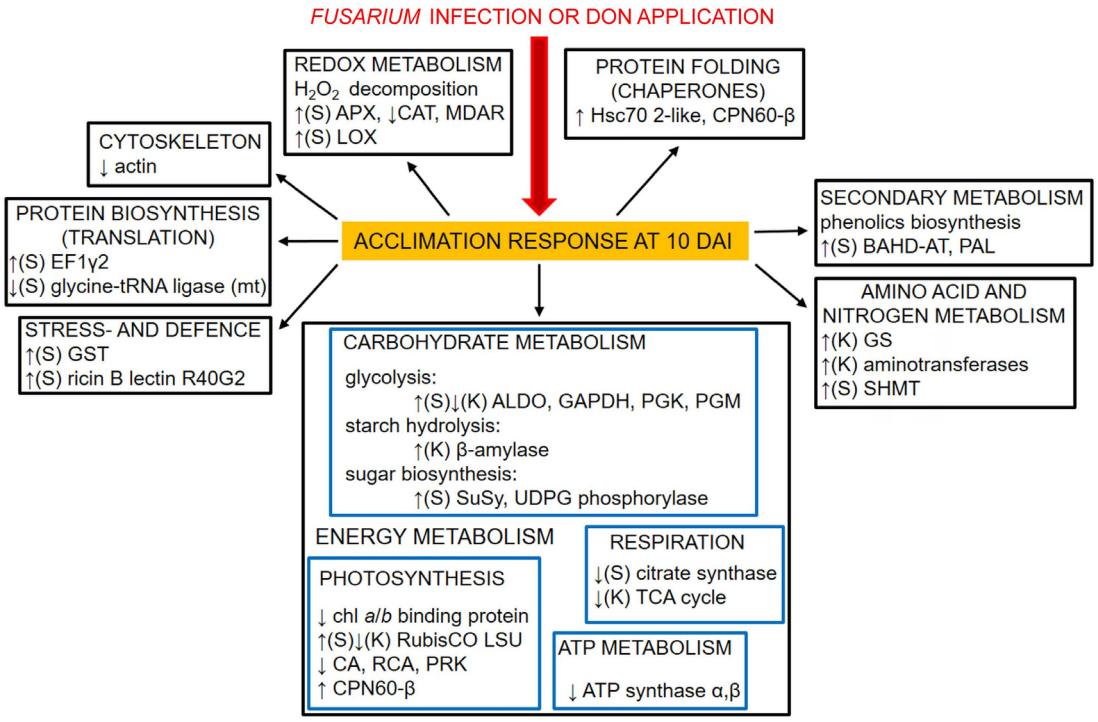

Fig. 6. A scheme summarising major protein functional classes affected by *Fusarium*- or DON treatments in Sumai 3 (S) and SW Kadrilj (K) spikes 10 dai. *Arrows* (↑) indicate an increased protein rel. abundance while (↓) indicate a decreased protein rel. abundance in *Fusarium*- or DON-treated plants with respect to untreated ones (control). Abbreviations: ALDO - aldolase; APX - ascorbate peroxidase; BAHD-AT - BAHD acyltransferase; CA - carbonic anhydrase; CAT - catalase; dai - days after inoculation; EF1γ2 - elongation factor 1γ2; GAPDH - glyceraldehyde-3-phosphate dehydrogenase; GS - glutamine synthase; GST - glutathione-S-transferase; Hsc70 - heat shock cognate protein 70; LOX - lipoxygenase; MDAR - monodehydroascorbate reductase; mt - mitochondrial isoform; PAL - phenylalanine ammonia lyase; PGK - phosphoglycerate kinase; PGM - 2,3-bisphosphate phosphoglycerate mutase; PRK - phosphoribulokinase; RCA - RubisCO activase A; RubisCO LSU - ribulose-1,5-bisphosphate carboxylase/oxygenase large subunit; SHMT - serine hydroxymethyltransferase; SuSy - sucrose synthase; TCA - tricarboxylic acid cycle; UDPG phosphorylase - UTP - glucose-1-phosphate uridylyltransferase.

decrease in *Fusarium*-treated and DON-treated plants with respect to control in both Sumai and Kadrilj plants at 10 dai. The obtained results correspond with the findings of Leontovyčová *et al.* (2019) that disruption and depolymerization of actin cytoskeleton could lead to enhanced plant resistance to pathogens via an activation of isochorismate synthase (ICS)-dependent SA biosynthetic pathway. The researchers have found out that application of actin depolymerizing drugs in *A. thaliana* treated with bacterial pathogen *Pseudomonas syringae* and *Brassica napus* treated with fungal pathogen *Leptosphaeria maculans* led to an activation of ICS-dependent SA biosynthetic pathway resulting in enhanced plant resistance to pathogen. In our study aimed at an investigation of total proteome in wheat spikes treated with *Fusarium culmorum* or mycotoxin DON at 10 dai, actin depolymerization was most probably followed by actin monomer degradation resulting in decreased actin content in *Fusarium*- and DON-treated wheats at 10 dai. Our results thus correspond with the findings by Leontovyčová *et al.* (2019) indicating a general mechanism of actin cytoskeleton disruption in induction of plant resistance against pathogens. Moreover, alterations in actin isoforms AtACT2 and AtACT7 were recently observed in *A. thaliana* in response to stress resulting in a decrease in thinner filaments formed by AtACT2 while an increase in thicker filaments formed by AtACT7 isoform (Kijima *et al.* 2018). Therefore, a decrease in actin 1 and actin 3 isoforms in *Fusarium*- and DON-treated wheat spikes may be a part of actin cytoskeleton reorganization under pathogen infection.

Comparison of our results to similar studies: Similarities were found between our study and the study by Ding *et al.* (2017) on Sumai 3 (resistant) and Huaimai 27 (susceptible) young spikes which were inoculated with *F. graminearum* (FHB) *vs.* water (control), and sampled at 1 dai for 2-DE proteomic analysis. In both studies, the following proteins were found increased in response to *Fusarium* infection: glutamine synthetase GS1b, phenylalanine ammonia lyase (PAL) (only in Sumai); small heat shock protein Hsp23.6 (in both genotypes); downregulated proteins: RubisCO activase, ATP synthase δ chain, vacuolar proton-ATPase subunit A; 3-isopropylmalate dehydratase large subunit (only in susceptible genotype), catalase-I, translation elongation factor Tu (in both genotypes). The major difference lies in sampling time which was 1 dai (alarm phase) in the study by Ding *et al.* (2017) while 10 dai (full acclimation to *Fusarium* inoculation and DON treatment) in our study. Since Ding *et al.* (2017) studied spike response to *Fusarium* at 1 dai, *i.e.,* very early stage of stress response, they were able to identify several proteins involved in signalling pathways (serine/threonine protein kinase, protein phosphatase 2C, serine/threonine phosphatase type 2c) while in our study, an acclimation response at 10 dai was observed. In contrast, our study performed at 10 dai shows that acclimation response was associated with profound alterations in cellular metabolism, namely energy metabolism as well as biosynthesis of several protective proteins and metabolites in resistant Sumai (lectins and other glycoproteins - enhanced content of sucrose synthase and UDP-glucose-1-phosphate uridylyltransferase; phenolic compounds - enhanced phenylalanine ammonia lyase and BAHD acyltransferase) and some results might also indirectly indicate alterations in the biosynthesis of pathogen-responsive phytohormones JA (LOX) and SA (PAL). A role of JA-SA crosstalk in *A. thaliana* response to *Fusarium graminearum* was studied by Makandar *et al.* (2010) who reported a role of SA in acquisition of plant systemic acquired resistance while JA signalling rather seems to contribute to plant susceptibility to the pathogen. However, an enhanced susceptibility of *A. thaliana* double mutant in JA biosynthetic pathway indicates an ambiguous role of JA in plant defense against pathogen.

A comparison of the currently identified DAPs with our previous study on *Fusarium*- and DON-treated spikes of barley c*vs.* Chevron and Pedant sampled at 10 dai (Kosová *et al.* 2017) revealed important differences in functional categories of the identified DAPs. Among barley DAPs, the most abundant categories involve „carbohydrate metabolism“ and „storage proteins“ indicating enhanced biosynthesis of carbohydrates and storage proteins in mature grains. Among wheat DAPs, the most abundant functional categories included „amino acid metabolism“, „carbohydrate metabolism“, and „photosynthesis-related proteins“ indicating that wheat spikes were still green with active photosynthesis. It can thus be concluded that barley cultivars revealed faster development of their spikes from flowering to grain maturity than the wheat cultivars employed in the present study.

Conclusions

In a summary, our study provides an insight into an acclimation response to *F. culmorum* inoculation and DON application in wheat cultivars with contrasting FHB resistance, *i.e.*, Sumai 3 as a resistance source *vs.* SW Kadrilj as an FHB-susceptible cultivar. Enhanced resistance of Sumai 3 is reflected by significantly lower level of DON content in mature grains in both *Fusarium*- and DON-treated plants with respect to SW Kadrilj. At proteome level, enhanced resistance of Sumai 3 is associated with relatively enhanced content of crucial enzymes of energy metabolism such as some glycolytic enzymes (ALDO, GAPDH) and photosynthetic enzymes such as RubisCO LSU enabling the genotype to activate metabolic pathways leading to an active acclimation to the pathogen, *i.e.*, biosynthesis of specific sugar-containing compounds (glycolipids and glycoproteins such as lectins) and phenolic compounds with protective functions. Enhanced abundances of enzymes involved in biosynthesis of cell wall related phenolic compounds were found as a specific plant response to pathogen inoculation only while no such response to sole mycotoxin application was found.

References

Anderson, J.A., Stack R.W., Liu S., Waldron, B.L., Fjeld, A.D., Coyne, C., Moreno-Sevilla, B., Mitchell Fetch, J., Song, Q.J., Cregan, P.B., Frohberg, R.C.: DNA markers for *Fusarium* head blight resistance QTLs in two wheat populations. - Theor. appl. Genet. **102**: 1164-1168, 2001.

Bontpart, T., Cheynier, V., Ageorges, A., Terrier, N.: BAHD or SCPL acyltransferase? What a dilemma for acylation in the world of plant phenolic compounds. - New Phytol. **208**: 695-707, 2015.

Buerstmayr, H., Lemmens, M., Hartl, L., Doldi, L., Steiner, B., Stierschneider, M., Ruckenbauer, P.: Molecular mapping of QTL for *Fusarium* head blight resistance in spring wheat. I. Resistance to fungal spread (Type II resistance). - Theor. appl. Genet. **104**: 84-91, 2002.

Buerstmayr, H., Steiner, B., Hartl, L., Griesser, M., Angerer, N., Lengauer, D., Miedaner, T., Schneider, B., Lemmens, M.: Molecular mapping of QTLs for *Fusarium* head blight resistance in spring wheat. II. Resistance to fungal penetration and spread. - Theor. appl. Genet. **107**: 503-508, 2003.

Caraux, G., Pinloche, S.: Permutmatrix: a graphical environment to arrange gene expression profiles in optimal linear order. - Bioinformatics **21**: 1280-1281, 2005.

Chambers, J.K., Macdonald, L.E., Sarau, H.M., Ames, R.S., Freeman, K., Foley, J.J. et al.: A G protein-coupled receptor for UDP-glucose. - J. biol. Chem. **275**: 10767-10771, 2000.

Chetouhi, C., Bonhommeee L., Lecomte P., Cambon F., Merlino M., Biron, D.G., Langin, T.: A proteomics survey on wheat susceptibility to *Fusarium* head blight during grain development. - Eur. J. Plant Pathol. **141**: 407-418, 2015.

Chivasa, S., Tomé, D., Slabas, A.: UDP-glucose pyrophosphorylase is a novel plant cell death regulator. - J. Proteome Res. **12**: 1743-1753, 2013.

Chrpová, J., Šíp, V., Štočková, L., Stemberková, L., Tvarůžek, L.: Resistance to *Fusarium* head blight in spring barley. - Czech J. Genet. Plant Breed. **47**: 58-63, 2011.

Cuthbert, P.A., Somers, D.J., Thomas, J., Cloutier, S., Brule-Babel, A.: Fine mapping *Fhb1*, a major gene controlling *Fusarium* head blight resistance in bread wheat (*Triticum aestivum* L.). - Theor. appl. Genet. **112**: 1465-1472, 2006.

Ding, L.N., Xu, H.B., Yi, H.Y., Yang, L.M., Kong, Z.X., Zhang, L.X., Xue, S.L., Jia, H.Y., Ma, Z.Q.: Resistance to hemi-biotrophic *F. graminearum* infection is associated with coordinated and ordered expression of diverse defense signaling pathways. - PLoS ONE **6**: e19008, 2011.

Ding, L., Yang, R., Yang, G., Cao, J., Li, P., Zhou, Y.: Identification of putative phosphoproteins in wheat spikes induced by *Fusarium graminearum*. - Planta **243**: 719-731, 2016.

Ding, L., Li, M., Li, P., Cao, J.: Comparative proteomics analysis of young spikes of wheat in response to *Fusarium graminearum* infection. - Acta Physiol. Plant. **39**: 271, 2017.

Eggert, K., Pawelzik, E.: Proteome analysis of *Fusarium* head blight in grains of naked barley (*Hordeum vulgare* subsp. *nudum)*. - Proteomics **11**: 972-985, 2011.

Eggert, K., Zörb, C., Mühling, K.H., Pawelzik, E.: Proteome analysis of *Fusarium* infection in emmer grains (*Triticum dicoccum*). - Plant Pathol. **60**: 918-928, 2011.

Glickman, M.H., Klinman, J.P.: Lipoxygenase reaction mechanism: demonstration that hydrogen abstraction from substrate precedes dioxygen binding during cartalytic turnover. - Biochemistry **35**: 12882-12892, 1996.

Gunnaiah, R., Kushalappa, A.C., Duggavathi, R., Fox, S., Somers, D.J.: Integrated metabolo-proteomic approach to decipher the mechanisms by which wheat QTL (Fhb1) contributes to resistance against *Fusarium graminearum*. - PLoS ONE **7**: e40695, 2012.

He, Y., Mawhinney, T.P., Preuss M.L., Schroeder, A.C., Chen, B., Abraham, L., Jez, J.M., Chen, S.: A redox-active isopropylmalate dehydrogenase functions in the biosynthesis of glucosinolates and leucine in *Arabidopsis*. - Plant J. **60**: 679-690, 2009.

Janse van Rensburg. H.C., Van den Ende, W.: UDP-glucose: a potential signaling molecule in plants? - Front. Plant Sci. **8**: 2230, 2018.

Kijima, S.T., Staiger, C.J., Katoh, K., Nagasaki, A., Ito, K., Uyeda, T.Q.P.: *Arabidopsis* vegetative actin isoforms, AtACT2 and AtACT7, generate distinct filament arrays in living plant cells. - Sci. Rep. **8**: 4381, 2018.

Kosová, K., Chrpová, J., Šíp, V.: Cereal resistance to *Fusarium* head blight and possibilities of its improvement through breeding. - Czech J. Genet. Plant Breed. **45**: 87-105, 2009.

Kosová, K., Chrpová, J., Šantrůček, J., Hynek, R., Štěrbová, L., Vítámvás, P., Bradová, J., Prášil, I.T.: The effect of *Fusarium culmorum* infection and deoxynivalenol (DON) application on proteome response in barley cultivars Chevron and Pedant. - J. Proteomics **169**: 112-124, 2017.

Kosová, K, Vítámvás, P., Urban, M.O., Prášil, I.T., Renaut, J.: Plant abiotic stress proteomics: the major factors determining alterations in cellular proteome. - Front. Plant Sci. **9**: 122, 2018.

Lannoo, N., Van Damme, E.J.M.: Lectin domains at the frontiers of plant defense. - Front. Plant Sci. **5**: 397, 2014.

Lemmens, M., Scholz, U., Berthiller, F., Dall´Asta, C., Koutnik, A., Schuhmacher, R., Adam, G., Buerstmayr, H., Mesetrhazy, A., Krska, R., Ruckenbauer, R.: The ability to detoxify the mycotoxin deoxynivalenol colocalizes with a major quantitative trait locus for *Fusarium* head blight resistance in wheat. - Mol. Plant-Microbe Interact. **18**: 1318-1324, 2005.

Leontovyčová, H., Kalachova, T., Trdá, L., Pospíchalová, R., Lamparová, L., Dobrev, P.I., Malínská, K., Burketová, L., Valentová, O., Janda, M.: Actin depolymerization is able to increase plant resistance against pathogens via activation of salicylic acid signalling pathway. - Sci. Rep. **9**: 10397, 2019.

Li, W.L., Faris, J.D., Muthukrishnan, S., Liu, D.J., Chen, P.D., Gill, B.S.: Isolation and characterization of novel cDNA clones of acidic chitinases and β-1,3-glucanases from wheat spikes infected by *Fusarium graminearum*. - Theor. appl. Genet. **102**: 353-362, 2001.

Lionetti, V., Giancaspro, A., Fabri, E., Giove, S.L., Reem, N., Zabotina, O.A., Blanco, A., Gadaleta, A., Bellincampi, D.: Cell wall traits as potential resources to improve resistance of durum wheat against *Fusarium graminearum*. - BMC Plant Biol. **15**: 6, 2015.

Liu, J.J., Li, L., Foroud, N.A., Gong, X., Li, C.C., Li, T.: Proteomics of bulked rachides combined with documented QTL uncovers genotype nonspecific players of the *Fusarium* head blight responses in wheat. - Phytopathology **109**: 111-119, 2019.

Maalekuu, K., Elkind, Y., Leikin-Frenkel, A., Lurie, S., Fallik, E.: The relationship between water loss, lipid content, membrane integrity and lox activity in ripe pepper fruit after storage. - Postharvest Biol. Technol. **42**: 248-255, 2006.

Makandar, R., Naiam, V., Chaturvedi, R., Jeannotte, R., Sparks, A.A., Shah, J.: Involvement of salicylate and jasmonate signaling pathways in *Arabidopsis* interaction with *Fusarium graminearum*. - Mol. Plant Microbe Interact. **23**: 861-870, 2010.

Mesterházy, A.: Types and components of resistance to *Fusarium* head blight of wheat. - Plant Breed. **114**: 377-386, 1995.

Mesterházy, A.: Theory and practice of the breeding for *Fusarium*

head blight resistance in wheat. - J. appl. Genet. **43A**: 289-302, 2002.
Mesterházy, A., Tóth, B., Varga, M., Bartók, T., Szabó-Hevér, A., Farády, L., Lehoczki-Krsjak, S.: Role of fungicides, application of nozzle types, and the resistance level of wheat varieties in the control of *Fusarium* head blight and deoxynivalenol. - Toxins (Basel) **3**: 1453-1483, 2011.
Mugford, S.T., Qi, X., Bakht, S., Hill, L., Wegel, E., Hughes, R.K., Papadopoulou, K., Melton, R., Philo, M., Sainsbury, F., Lomonossoff G.P., Roy A.D., Goss R.J.M., Osbourn A.: A serine carboxypeptidase-like acyltransferase is required for synthesis of antimicrobial compounds and disease resistance in oats. - Plant Cell **21**: 2473-2484, 2009.
Noël, L.D., Cagna, G., Stuttmann, J., Wirthmüller, L., Betsuyaku, S., Witte, C.P., Bhat, R., Pochon, N., Colby, T., Parker, J.E.: Interaction between SGT1 and cytosolic/nuclear HSC70 chaperones regulates *Arabidopsis* immune responses. - Plant Cell **19**: 4061-4076, 2007.
Rawat, N., Pumphrey, M.O., Liu, S., Zhang, X., Tiwari, V.K., Ando, K., Trick, H.N., Bockus, W.W., Akhunov, E., Anderson, J.A., Gill, B.S.: Wheat *Fhb1* encodes a chimeric lectin with agglutinin domains and a pore-forming toxin-like domain conferring resistance to *Fusarium* head blight. - Nature Genet. **48**: 1576-1580, 2016.
Shahidi-Noghabi, S., Van Damme, E.J.M., Smagghe, G.: Carbohydrate-binding activity of the type-2 ribosome-inactivating protein SNA-I from elderberry (*Sambucus nigra*) is a determining factor for its insecticidal activity. - Phytochemistry **69**: 2972-2978, 2008.
Siedow, J.N.: Plant lipoxygenase: structure and function. - Annu. Rev. Plant Physiol. Plant mol. Biol. **42**: 145-188, 1991.
Vančo, B., Šliková, S., Šudyová, V., Šrobárová, A.: Response to *Fusarium culmorum* inoculation in barley. - Biologia **62**: 56-61, 2007.
Waldron, B.L., Moreno-Sevilla, B., Anderson, J.A., Stack, R.W., Frohberg, R.C.: RFLP mapping of QTL for *Fusarium* head blight resistance in wheat. - Crop Sci. **39**: 805-811, 1999.
Wasternack, C., Hause, B.: Jasmonates: biosynthesis, perception, signal transduction and action in plant stress response, growth and development. An update to the 2007 review in Annals of Botany. - Ann. Bot. **111**: 1021-1058, 2013.
Wang, Y., Yang, L.M., Xu, H.B., Li, Q.F., Ma, Z.Q., Chu, C.G.: Differential proteomic analysis of proteins in wheat spikes induced by *Fusarium graminearum*. - Proteomics **5**: 4496-4503, 2005.
Wang, W., Vignani, R., Scali, M., Cresti, M.: A universal and rapid protocol for protein extraction from recalcitrant plant tissues for proteomic analysis. - Electrophoresis **27**: 2782-2786, 2006.
Yang, F., Jensen, J.D., Svensson, B., Jørgensen, H.J.L., Collinge, D.B., Finnie, C.: Analysis of early events in the interaction between *Fusarium graminearum* and the susceptible barley (*Hordeum vulgare*) cultivar Scarlett. - Proteomics **10**: 3748-3755, 2010a.
Yang, F., Jensen, J.D., Spliid, N.H., Svensson, B., Jacobsen, S., Jørgensen, L.N., Jørgensen, H.J.L., Collinge D.B., Finnie C.: et al.: Investigation of the effect of nitrogen on severity of *Fusarium* Head Blight in barley. - J. Proteomics **73**: 743-752, 2010b.
Yang, F., Jacobsen, S., Jorgensen, H.J.L., Collinge, D.B., Svensson, B., Finnie, C.: *Fusarium graminearum* and its interactions with cereal heads: studies in the proteomics era. - Front. Plant Sci. **4**: 37, 2013.
Zhou, W., Eudes, F., Laroche, A.: Identification of differentially regulated proteins in response to a compatible interaction between the pathogen *Fusarium graminearum* and its host, *Triticum aestivum*. - Proteomics **6**: 4599-4609, 2006.
Zhou, W., Kolb, F.L., Riechers, D.E.: Identification of proteins induced or upregulated by *Fusarium* head blight infection in the spikes of hexaploid wheat (*Triticum aestivum*). - Genome **48**: 770-780, 2005.